The effect of the crystal electric field on the Kondo-type fluctuations in $YbAuCu_4$

1996 J. Phys.: Condens. Matter 8 7755

(http://iopscience.iop.org/0953-8984/8/41/020)

J. Phys.: Condens. Matter **8** (1996) 7755–7770. Printed in the UK

The effect of the crystal electric field on the Kondo-type fluctuations in $YbAuCu_4$

P Bonville†, P Dalmas de Réotier‡, A Yaouanc‡, G Polatsek§,
P C M Gubbens‖ and A M Mulders‖

† Commissariat à l'Energie Atomique, Département de Recherche sur l'Etat Condensé, les Atomes et les Molécules, F-91191 Gif-sur-Yvette, France

‡ Commissariat à l'Energie Atomique, Département de Recherche Fondamentale sur la Matière Condensée, F-38054 Grenoble Cédex 9, France

§ Institut für Theoretische Physik, Technische Universität, Mommsen Strasse 13, 01069 Dresden, Germany

‖ Interfacultair Reactor Instituut, Delft University of Technology, 2629 JB Delft, The Netherlands

Received 24 May 1996, in final form 2 August 1996

Abstract. We present a positive-muon spectroscopy (μSR) study of the cubic Kondo lattice $YbAuCu_4$, where the crystal-field splittings of the Yb^{3+} ion amount to a few tens of K. The transition from the paramagnetic to the antiferromagnetic state is detected at $T \sim 0.5$ K. The zero-field data provide evidence of an unusual temperature dependence of the mean nuclear dipole field at the muon site. The longitudinal μSR relaxation rate as well as the published quasi-elastic neutron linewidth, both recorded far into the paramagnetic region ($T \gtrsim 20$ K), are analysed in detail. We show that the classical kf exchange interaction cannot explain the observed thermal variation of the dynamical μSR and neutron widths. We perform a calculation of the 4f excitation spectra using the $1/N_f$ expansion, applied to the Anderson one-impurity Hamiltonian in the non-crossing approximation (NCA), in the presence of crystal-field splittings, and compare the results with the observed thermal variations of the dynamical widths. Whereas the NCA reasonably explains the neutron measurements, it strongly overestimates the low-temperature μSR width. We discuss different possible reasons for this discrepancy.

1. Introduction

Positive-muon spectroscopy (μSR) is becoming an increasingly popular tool for investigating the magnetic properties of solids at a microscopic level [1], along with more classical methods such as neutron scattering, nuclear magnetic resonance (NMR) and Mössbauer spectroscopy. Both the static and dynamic aspects of electronic magnetism can be probed by the μSR technique. As regards dynamics, the measurement of the electronic fluctuation frequencies by μSR is based on the observation of the depolarization of the initially 100% spin-polarized muon beam by the internal fluctuating electronic fields [1]. It offers the advantage of a wide accessible-frequency range (0.1 MHz–50 GHz), with the relative drawback that the determination of the muon stopping site(s) in the material is often difficult. However, as we shall see, using symmetry arguments, quantitative information can be extracted from the measured time evolution of the depolarization.

In Ce- or Yb-based intermetallics, the presence of hybridization between localized 4f and itinerant conduction electrons leads to peculiar properties such as the Kondo effect, the intermediate-valence state or 'heavy-electron' behaviour [2]. In Kondo lattices, i.e. materials

0953-8984/96/417755+16$19.50

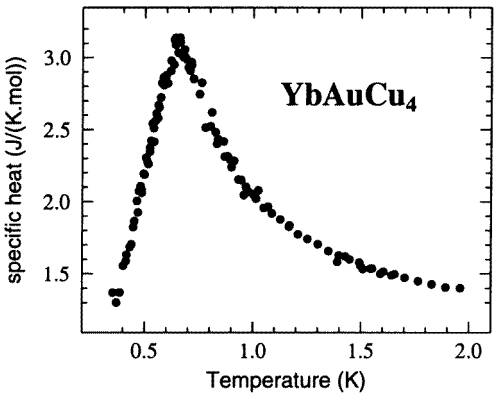

Figure 1. The specific heat anomaly in $YbAuCu_4$ at the magnetic transition.

with weak hybridization, the conduction-electron-driven fluctuation rate of the rare-earth magnetic moment has been predicted to follow approximately a $T^{1/2}$-law for $T \gtrsim 5\ T_0$ [3], where T_0 is the Kondo temperature, instead of the linear Korringa law observed for metallic paramagnets free from hybridization. Such a law is expected to hold for a degenerate Kondo ion, i.e. in the absence of sizeable crystal-field splittings, and evidence of its validity has been obtained for several Ce-based and in a few Yb-based Kondo lattices from inelastic neutron scattering spectroscopy [4, 5] and NMR measurements [6, 7]. The bulk of the μSR studies of these materials have focused on the low-temperature properties in the search for very small magnetic moments [8, 9].

In this work, we present a μSR study of the cubic Kondo lattice $YbAuCu_4$. In this compound, the Yb^{3+} sublattice orders magnetically (with probably an antiferromagnetic structure) at low temperature; the value of the transition temperature T_N is 0.6 K according to specific heat data (reference [10] and figure 1) and $\simeq$1 K according to ^{170}Yb Mössbauer measurements [11]. The latter allowed the saturated spontaneous Yb^{3+} magnetic moment to be determined: $m_{\rm sp} = 1.45\ \mu_B$. The cubic crystal-electric-field (CEF) interaction splits the $J = 7/2$ ground spin–orbit multiplet of the Yb^{3+} ion. Its CEF level scheme in $YbAuCu_4$, as determined by inelastic neutron scattering [12], is the following: the Γ_7 doublet is the ground state, the Γ_8 quartet and the Γ_6 doublet lying respectively at $\sim$45 K and $\sim$80 K above the ground state. The measured saturated spontaneous moment (1.45 μ_B) is reduced with respect to the bare Γ_7 moment (1.715 μ_B), which is attributed to the Kondo coupling.

The organization of this paper is as follows. In section 2, we present the experimental μSR data. In section 3 we discuss the meaning of the μSR relaxation rate data and in section 4 we perform a tentative analysis of these data and of the published quasi-elastic neutron results [12] in terms of the Kondo coupling on the Yb^{3+} ion. Section 5 contains the discussion of the results, and section 6 the conclusion.

2. Experimental results

The compound $YbAuCu_4$ crystallizes into a cubic fcc structure (space group $F\bar{4}3m$), with a room temperature lattice parameter $a \simeq 7.05$ Å. Our sample is an ingot melted in an arc furnace; an x-ray diffractogram showed the presence of $\simeq$10% metallic Cu beside the main phase. The magnetic susceptibility exhibits a Curie–Weiss law above 100 K with $\mu_{\rm eff} = 4.4\ \mu_B$ (close to the Yb^{3+} free-ion effective moment of 4.54 μ_B) and $\Theta_p = -11$ K, indicative

of antiferromagnetic interactions.

The μSR sample was made of slices 1 mm thick cut from the original ingot and glued onto a silver plate. The sample diameter was ~25 mm.

The μSR experiments were performed with the MuSR spectrometer of the ISIS surface muon beam facility located at the Rutherford Appleton Laboratory (UK) [13]. The spectra were recorded with the longitudinal geometry, in zero magnetic field and in applied fields of 20 mT and 200 mT, and with temperatures between 0.1 K and 280 K. Experiments below 2 K were carried out in a ^{3}He–^{4}He dilution refrigerator.

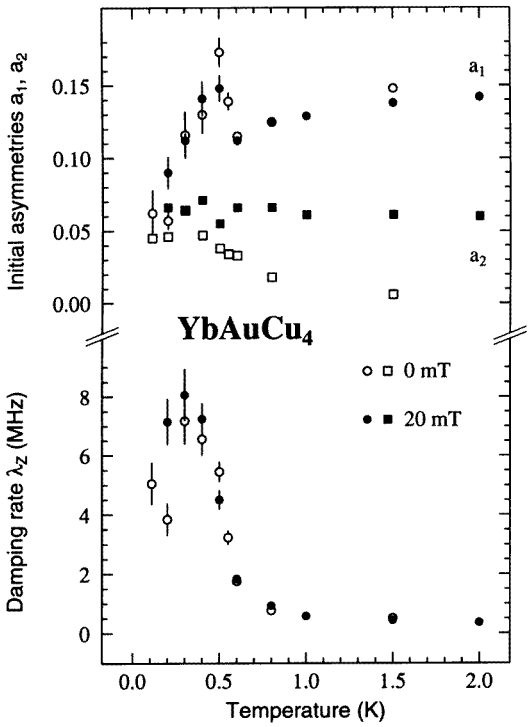

Figure 2. The low-temperature dependence of the asymmetries a_1 (circles) and a_2 (squares) and damping rate λ_Z (circles) for a polycrystalline $YbAuCu_4$ sample extracted from spectra recorded in zero field (open symbols) and in a longitudinal field of 20 mT (filled symbols). The data indicate that the magnetic phase transition occurs at $T_N \sim 0.5$ K.

A μSR measurement consists in recording the spin-depolarization function $P_Z(t)$ which reflects the evolution of the field at the muon site. The Z-axis refers to the muon beam polarization axis which, in our case, is the direction of the detected positrons as well, because all of our measurements have been performed with the longitudinal geometry [1].

2.1. Low-temperature measurements

The spectra at low temperature ($T < 4.5$ K) show a monotonically rapid decay of the muon polarization. Below T_N we do not observe any oscillations either because they are too much damped or they cannot be resolved at ISIS [13]. An approximate description of the decay is obtained with the law

$$a P_Z(t) = a_1 \exp(-\lambda_Z t) + a_2 + a_{\mathrm{Ag}} \tag{1}$$

where a, a_1, a_2 and a_{Ag} are amplitudes (or asymmetries) and λ_Z a damping rate which describes how the muon is depolarized by the magnetic fluctuations; a_{Ag} accounts for the fraction of muons stopped in the silver backing plate and it is estimated from calibration transverse-field spectra to be ∼0.03. The thermal variations of $a_1(T)$, $a_2(T)$, and $\lambda_Z(T)$ are presented in figure 2. $a_1(T)$ shows an anomaly at 0.5 K and decreases for $T \lesssim 0.5$ K, and $\lambda_Z(T)$ exhibits a maximum at around 0.4 K. These features are associated with the presence of the magnetic transition at $T_N \sim 0.5$ K. The increase of λ_Z as the temperature approaches T_N from above is due to the slowing down of the Yb^{3+} magnetic fluctuations.

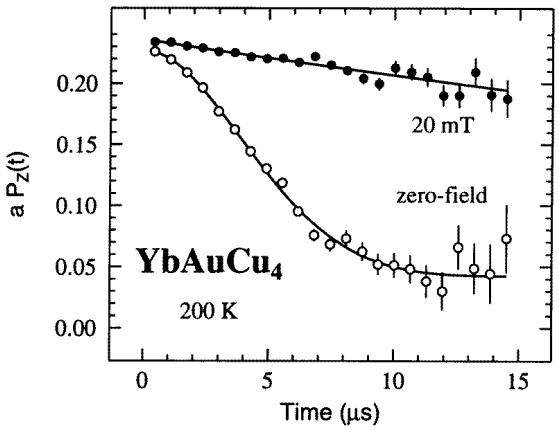

Figure 3. Time evolution of the μSR depolarization recorded in $YbAuCu_4$ at $T = 200$ K, characteristic of the spectra obtained for $T \geqslant 20$ K, in zero field and with a longitudinal field of 20 mT; the solid lines are fits to the product of an exponential and a dynamical Kubo–Toyabe lineshape for the zero-field signal, and to an exponential decay for the 20 mT signal. For each spectrum a constant term (∼0.03) accounts for the muons stopped in the silver backing plate. Note the strong field dependence of the shape of the spectra.

As to the undamped component a_2, in zero field it vanishes above 2 K, increases as the temperature decreases and seems to level off below ∼0.5 K. In a 20 mT longitudinal field, a_2 is temperature independent below 2 K (≃0.06). Between 2 K and 20 K, a_2 progressively decreases to 0 while a_1 slightly increases. We have at present no explanation for the complex behaviour of $a_2(T)$. We note that the zero-field spectra are poorly fitted by equation (1), which is used merely as a practical way to display the data. The spectra with a longitudinal field of 20 mT are well described by equation (1) below 20 K, but, because of the presence of the term $a_2(T)$, the depolarization function cannot be considered to be a simple exponential decay. Although the physical case is different, the thermal behaviour of $a_2(T)$ is reminiscent of what has been observed for magnetic quasi-crystals [14].

2.2. High-temperature longitudinal-field measurements

We present here the data recorded for $T > 20$ K with a longitudinal magnetic field. Whereas at low temperature, application of a longitudinal field does not drastically alter $P_Z(t)$, at high temperature, the field has a strong effect on the depolarization function (see figure 3). In applied fields of 20 mT and 200 mT the spectra are true exponential depolarization functions, i.e. the amplitude a_1 of equation (1) is temperature independent with the standard value $a_1 \simeq 0.20$ ($a_2 = 0$). The spectra yield λ_Z-values which decrease monotonically as temperature increases as shown in figure 4. Interestingly λ_Z is field independent. As

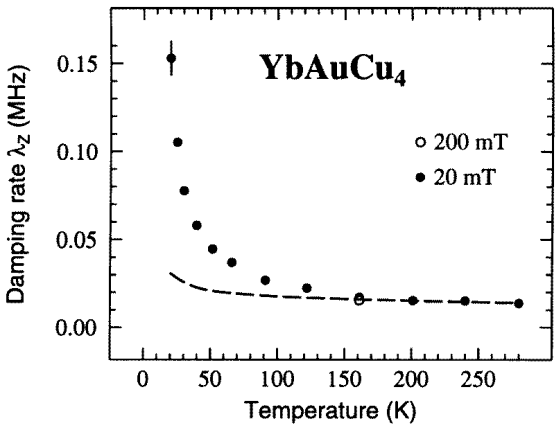

Figure 4. The temperature dependence of the μSR relaxation rate $\lambda_Z(T)$ measured in longitudinal magnetic fields for $T \geqslant 20$ K in $YbAuCu_4$; λ_Z probes the Yb^{3+} paramagnetic fluctuations. The dashed line is the prediction of the NCA calculation for single-site fluctuations of the localized Yb^{3+} magnetic moment assumed to be at a cubic site (see the text).

the nuclear spins are well decoupled by the longitudinal field (see the next section), the muon depolarization observed in longitudinal fields is solely due to the electronic magnetic fluctuations. In this temperature range ($T > 20$ K, i.e. $T > 40\ T_N$), it is probably a good approximation to neglect the intersite correlations between the Yb^{3+} total angular momenta. These data will be interpreted with a single-ion fluctuation model in section 3.

We note that metallic Cu contained in our sample does not influence the spectra recorded in longitudinal fields because the Cu nuclear magnetic moments are decoupled by the field.

2.3. Zero-field high-temperature measurements

In order to get information about the muon stopping site and about an eventual diffusion in $YbAuCu_4$, we have performed zero-field measurements for $T \geqslant 20$ K.

The observed depolarization in zero field is mainly due to the nuclear moments contained in the compound (isotopes ^{63}Cu, ^{65}Cu, ^{171}Yb, ^{173}Yb and ^{197}Au). In addition, we have to take into account the contribution of the fluctuating 4f moments that we have unravelled at high fields. Therefore the compound depolarization function must be a product of two functions, each describing one depolarization channel. In fact all of the recorded spectra are well analysed by the function

$$a P_Z(t) = a_1 P_{\mathrm{KT}}(t) \exp(-\lambda_Z t) + a_{\mathrm{Ag}} \tag{2}$$

where $P_{\mathrm{KT}}(t)$ is the static Kubo–Toyabe decay:

$$P_{\mathrm{KT}}(t) = \frac{1}{3} + \frac{2}{3}(1 - \Delta_{\mathrm{n}}^2 t^2) \exp\left(-\frac{1}{2}\Delta_{\mathrm{n}}^2 t^2\right) \tag{3}$$

where $\Delta_{\mathrm{n}} = \gamma_\mu \sqrt{\langle B_n^2 \rangle}$ describes the width of the distribution of fields at the muon site due to the nuclear moments and γ_μ is the muon gyromagnetic ratio (γ_μ = 851.6 Mrad s^{-1} T^{-1}). The function in equation (3) accounts for the depolarization due to static nuclear moments; actually, the observed signal is better reproduced by a weakly dynamic Kubo–Toyabe lineshape with a small correlation frequency $\nu \simeq 0.1$ MHz [1]. A sample fit is shown in figure 3.

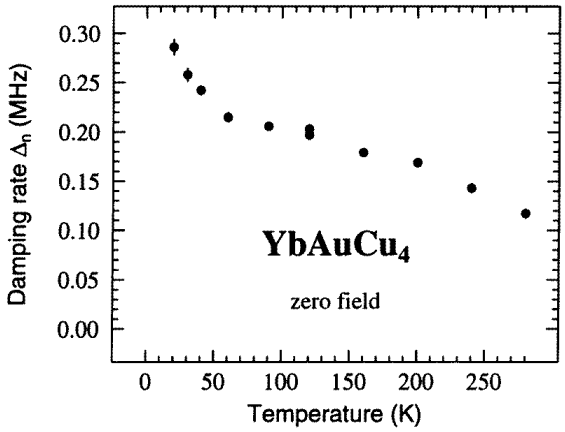

Figure 5. The temperature dependence of the zero-field depolarization rate Δ_n measured for $YbAuCu_4$ for $T \geqslant 20$ K; Δ_n is expected to be temperature independent. The observed thermal variation may originate from the temperature dependence of the electric field gradient acting at the Cu sites.

In figure 5 we present the measured value of Δ_n as a function of temperature obtained from the fit to the zero-field spectra, the value of λ_Z being fixed to the value obtained in a longitudinal-field spectrum recorded at the same temperature. The observed temperature dependence of Δ_n is unusual and cannot be attributed to the diffusion of the muon between different sites because the Gaussian shape at small times in the recorded spectra points to a static or very slowly diffusing muon at all temperatures. The quantity Δ_n can be computed if one assumes a realistic stopping site for the muon. We have found two possible sites in the crystal structure of $YbAuCu_4$. In Wyckoff notation they are sites 4b and 4d of coordinates (1/2, 1/2, 1/2) and (3/4, 3/4, 3/4), respectively. Neglecting in a first step the effect of the electric field gradient produced by the muon electric charge and by the Cu environment on the Cu nuclei (Cu is not at a cubic-symmetry crystallographic site), we obtain $\Delta_n \simeq 0.58$ MHz for the two sites from standard theory [1]. This value is larger than the low-temperature experimental value by a factor $\sim$2.5 and, additionally, the observed thermal dependence of Δ_n cannot be explained by the standard theory of the coupling of the muon spin with the nuclear spins, which yields a temperature-independent Δ_n. A possible explanation of this result can be found in the dependence of the dipole magnetic field at the muon site, on the electric field gradient acting on the nuclei [15]. Since the electronic properties of $YbAuCu_4$ are strongly temperature dependent, and the band electrons have a pronounced d character, thus being sensitive to the crystal field, it is conceivable that the electric field gradient due to the conduction electrons be also temperature dependent. This may provide an explanation for the temperature variation shown in figure 5. A meaningful quantitative analysis would require us to have zero-field and transverse-field data recorded on a single crystal.

Although we could not give a thorough quantitative interpretation of the zero-field data, it is clear that they do show that the muon in $YbAuCu_4$ is static compared to the characteristic time of the Yb^{3+} electronic fluctuations. This means that the coupling between the muon spin and the Yb^{3+} total angular momenta is temperature independent. The whole analysis of the spin dynamics given below is based on this fact.

3. The μSR relaxation rate and characteristics of the Yb^{3+} spin dynamics

In this section we discuss our high-temperature longitudinal μSR relaxation rate data ($T \geqslant 20$ K) in relation to the characteristics of the spin dynamics of the Yb^{3+} ions.

Taking into account the facts that (i) the depolarization is well described by an exponential function, (ii) the Yb^{3+} ions in $YbAuCu_4$ are at sites of cubic symmetry and (iii) the correlations between magnetic moments at different sites are neglected (probably a good approximation at high temperature in $YbAuCu_4$ as the RKKY exchange interaction is very weak; $T_N \sim 0.5$ K), the following expression for λ_Z, derived in a previous paper [16], can be used in the case of a single-crystal sample:

$$\lambda_Z(\theta, \varphi) = \left[\sum_{\beta,\alpha} L_{\beta\alpha}(\theta, \varphi) M_{\alpha\beta}\right] \frac{1}{\Gamma_{\mu\mathrm{SR}}} \tag{4}$$

where $\Gamma_{\mu\mathrm{SR}}$ is a 'dynamical μSR linewidth', and $L(\theta, \varphi)$ and M are matrices describing the crystal orientation dependence of the damping rate and of the coupling between the muon spin and the total angular momentum of the Yb^{3+} ions, respectively. Expression (4) is valid in the 'extreme-narrowing' limit, which will be seen to hold in $YbAuCu_4$ above 20 K. In order to compute M, we have to specify the muon localization site; in $YbAuCu_4$ we found two possible sites (see subsection 2.3). Since these sites have cubic symmetry, the matrix M reduces to a scalar and, using the expression for the matrix elements of $L(\theta, \varphi)$ [16], λ_Z given in equation (4) turns out to be independent of the angles θ and φ:

$$\lambda_Z = 2\Delta_{\mathrm{e}}^2 \frac{1}{\Gamma_{\mu\mathrm{SR}}} \tag{5}$$

where $\Delta_{\mathrm{e}}^2 \equiv M_{xx} = M_{yy} = M_{zz}$. As our measurements have been carried out for a polycrystalline sample, we need to perform the spherical averaging of $\exp(-\lambda_Z t)$ over θ and φ. Since λ_Z is angle independent, $P_Z(t)$ is the same for measurements performed on single-crystal and polycrystalline samples.

The dynamical width $\Gamma_{\mu\mathrm{SR}}$ is related to the one-sided time Fourier transform of the imaginary part of the dynamical electronic susceptibility, $\chi''(\omega)$, taken at $\omega = 0$. It has been shown that [16]

$$\frac{1}{\Gamma_{\mu\mathrm{SR}}} = \frac{1}{\chi_C} \lim_{\omega \to 0} \frac{\chi''(\omega)}{\pi\omega} \tag{6}$$

where χ_C is the free-ion Curie susceptibility. For a degenerate 4f ion, i.e. in the absence of CEF splittings, $\Gamma_{\mu\mathrm{SR}}$ is equal to the quasi-elastic half-width Γ_Q, for the case where the 4f excitation spectrum is Lorentzian shaped, or close to Lorentzian. In the presence of CEF splittings, and assuming Lorentzian-shaped lines, $\Gamma_{\mu\mathrm{SR}}$ can be expressed in terms of the Curie and Van Vleck susceptibilities, χ_C^m and χ_{VV}^{nm} respectively [16]:

$$\frac{1}{\Gamma_{\mu\mathrm{SR}}} = \frac{1}{\chi_C} \left\{ \sum_m \frac{\chi_C^m}{\Gamma_m} + \frac{1}{2} \sum_{m \neq n} \chi_{VV}^{nm} \left[1 - \exp(-\beta\Delta_{nm})\right] \frac{\Gamma_{nm}}{\Gamma_{nm}^2 + \Delta_{nm}^2/\hbar^2} \right\}. \tag{7}$$

The sums are over the CEF levels. Γ_m and Γ_{nm} are the dynamical linewidths of the m elastic and nm inelastic excitations of energy E_m and E_n, respectively. We have defined $\Delta_{nm} = E_n - E_m$ and $\beta = 1/k_B T$.

In order to extract $\Gamma_{\mu\mathrm{SR}}$ from the experimental λ_Z-values with equation (5), and to compare it to theory via equation (6) or equation (7), the muon–4f coupling Δ_{e} must be estimated. Taking into account only the dipolar coupling between the muon and 4f spins, numerical calculations give $\Delta_{\mathrm{e}} = 166$ MHz and 208 MHz respectively for the two stopping

sites 4b and 4d discussed in subsection 2.3. As site 4b is characterized by the longest possible distances between the muon and the Yb ions, no sites for the muon can be found with Δ_e smaller that 166 MHz.

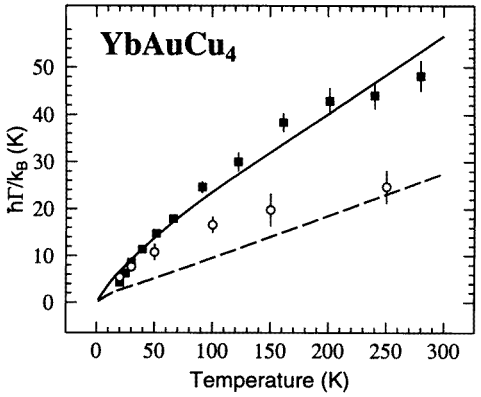

Figure 6. Thermal variations in $YbAuCu_4$ of the 4f μSR (solid symbols) and neutron (open circles) linewidths, $\Gamma_{\mu SR}$ and Γ_Q respectively; $\Gamma_{\mu SR}$ has been derived from the μSR λ_Z-data with a coupling constant Δ_e = 208 MHz; Γ_Q is taken from reference [12]. The solid and dashed lines show respectively $\Gamma_{\mu SR}$ and Γ_Q calculated on the assumption of a standard kf exchange interaction, with a coupling parameter $|J_{kf}n(E_F)| = 0.37$.

In figure 6 we have plotted $\Gamma_{\mu SR}(T)$ deduced from the measured $\lambda_Z(T)$-values making the hypothesis that the muon is localized in the 4d site (Δ_e = 208 MHz). The μSR width is seen to increase monotonically as temperature increases, and shows a $\sqrt{T}$-like saturation behaviour at high temperature. We have also reported in figure 6 the temperature dependence of the quasi-elastic linewidth Γ_Q measured in the inelastic neutron scattering experiments taken from reference [12]. In a first step towards interpretation, we have assumed that the 4f fluctuations are due to the classical kf exchange interaction with conduction electrons [17]. The quantities $\Gamma_{\mu SR}$ and Γ_Q then depend on a unique kf coupling parameter, $J_{kf}n(E_F)$, where J_{kf} is the conduction electron–4f-electron exchange integral and $n(E_F)$ is the metal density of electronic states at the Fermi energy per spin direction [16]. We find that the best fit to the experimental data is obtained with $|J_{kf}n(E_F)| = 0.37$. The theoretical curves are represented in figure 6 (the solid line for $\Gamma_{\mu SR}$ and the dashed line for Γ_Q); $\Gamma_Q(T)$ shows a T-linear Korringa behaviour above 20 K, whereas $\Gamma_{\mu SR}(T)$ has a pronounced curvature at low temperatures due to the progressive population of the CEF levels as temperature increases, and then shows a linear behaviour. It is clear from figure 6 that the classical kf exchange is not fully adequate to describe the experimental data. Although the low-temperature experimental behaviour of $\Gamma_{\mu SR}(T)$ is correctly reproduced, the observed curvature of $\Gamma_Q(T)$ and the high-temperature experimental variations of the two quantities, which are reminiscent of a $\sqrt{T}$-behaviour, do not match with the theoretical Korringa-type variation. The derived value of the kf coupling parameter (0.37) is also unrealistically high. The presence of the Kondo coupling in $YbAuCu_4$ is likely to influence the observed thermal variations of the dynamical widths. This will be discussed in section 4.

If we now consider the second possible occupation site for the muon (the 4b site, with Δ_e = 166 MHz), we find that the values of $\Gamma_{\mu SR}$ obtained from equation (5) are close to the experimental values of Γ_Q at high temperature. This is inconsistent with the general trend observed for the calculated curves of figure 6 (see also reference [16]), which show that

the high-temperature value of the $\Gamma_{\mu SR}/\Gamma_Q$ ratio should be close to 2 (for the case of a Γ_7 ground state). We believe therefore that site 4d (3/4, 3/4, 3/4) is the most likely stopping site for the muon in $YbAuCu_4$.

We can now address the validity of the 'extreme-narrowing' approximation. We have found experimentally that $P_Z(t)$ is an exponential function. As in NMR [18], this functional form is justified theoretically if the magnetic fluctuations are sufficiently fast, i.e. if $\Delta_e \ll \Gamma_{\mu SR}$, which is certainly valid in the paramagnetic phase of $YbAuCu_4$, where $\Delta_e \sim 0.2$ GHz and $\Gamma_{\mu SR} > 50$ GHz (see figure 6).

Another experimental finding is that λ_Z is field independent, for fields below 200 mT. This can be understood as follows. In the presence of a field, the Zeeman energies of the muon spin and of an Yb^{3+} total angular momentum, write $\hbar\omega_\mu = \hbar\gamma_\mu B_{ext}$ and $\hbar\omega_e = g\mu_B B_{ext}$, respectively. Then following standard NMR practice [18] we derive

$$\lambda_Z = \frac{2\Delta_e^2\Gamma_{\mu SR}}{\Gamma_{\mu SR}^2 + (\omega_\mu - \omega_e)^2.} \tag{8}$$

With B_{ext} = 200 mT, we have ω_μ = 27 MHz and $\omega_e \simeq 6$ GHz (for g = 2). So the following inequalities hold:

$$\omega_\mu \ll \omega_e \ll \Gamma_{\mu SR} \tag{9}$$

and thus the field-dependent term in the denominator of equation (8) can safely be neglected. The 4f relaxation rate could however be field dependent. This is not so in our case because an applied field of 200 mT is not expected to alter the spectral densities associated with conduction electron scattering above 4 K ($\hbar\omega_e/k_B \sim 0.3$ K $\ll T$), and is much lower than the crossover field $B_K \sim (k_B T_K)/(g\mu_B) \sim 0.75$ T (for T_K = 1 K, the low-temperature Kondo energy scale in $YbAuCu_4$; see section 4) above which the Kondo properties disappear.

4. Dynamical widths and Kondo coupling

Several measurements have provided evidence for the presence of the Kondo effect in $YbAuCu_4$, which manifests itself via anomalies in the electronic low-temperature properties. These anomalies consist in the reduction:

(i) of the specific heat jump at the magnetic transition [19], which in $YbAuCu_4$ is $\Delta C_p \simeq 2$ J K^{-1} mol^{-1} (reference [10] and figure 1) instead of $R\ln 2 = 5.76$ J K^{-1} mol^{-1} for a doublet ground state; and

(ii) of the saturated spontaneous Yb^{3+} moment, whose saturated value 1.45 μ_B [11] is lower than the bare Γ_7 moment value $m(\Gamma_7)$ = 1.715 μ_B.

The dynamical susceptibility for a single ion in the presence of the Kondo coupling has been obtained by treating the Anderson one-impurity model using the $1/N_f$ expansion technique in the self-consistent non-crossing approximation [3]. This calculation applies for a degenerate ion (N_f = 8 for Yb^{3+}), i.e. in the absence of CEF splittings, or in the presence of CEF splittings at sufficiently high temperature, such that $k_B T \gg \Delta_{nm}$. In the temperature range $T > 5T_0$, where T_0 is the Kondo temperature, the quasi-elastic dynamical width follows the empirical law

$$\Gamma(T) = \frac{2.4}{N_f}\frac{k_B T_0}{\hbar}\sqrt{\frac{T}{T_0}}. \tag{10}$$

At lower temperature, $\Gamma(T)$ goes through a minimum for $T \sim T_0$, then saturates towards a value $\Gamma(T \to 0) \sim k_B T_0/\hbar$ as T decreases. The experimental thermal variations of $\Gamma_{\mu SR}$

and Γ_Q do indeed show a $\sqrt{T}$-like variation at high temperature, but they clearly do not follow the expected behaviour for a degenerate ion at low temperature: both quantities decrease monotonically as temperature decreases. These effects are due to the presence of CEF splittings which are of the same order of magnitude as the Kondo temperature T_0.

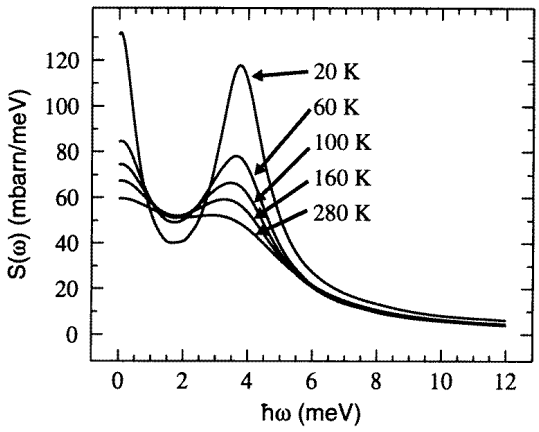

Figure 7. Inelastic neutron scattering spectra for the cubic CEF level scheme of $YbAuCu_4$ (Γ_7 ground state, Γ_8 at 45 K and Γ_6 at 80 K) computed with the NCA formalism for $T_0 = 20$ K at various temperatures. The inelastic line at $\simeq$4 meV corresponds to the $\Gamma_7 \rightarrow \Gamma_8$ transition, the $\Gamma_7 \rightarrow \Gamma_6$ transition being forbidden.

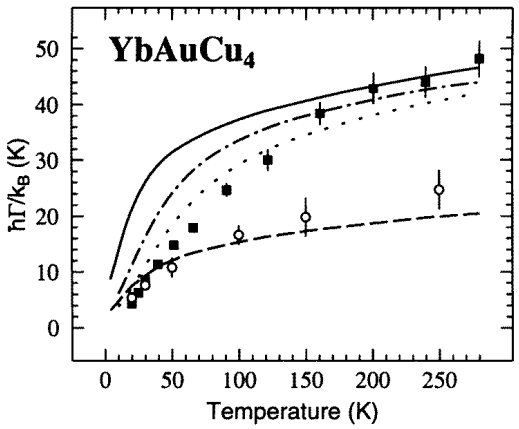

Figure 8. The same experimental data as in figure 6. The continuous ($\Gamma_{\mu SR}$) and dashed (Γ_Q) lines are the predictions of the NCA formalism with a Kondo 'high-temperature' scale $T_0 = 20$ K, assuming a cubic Yb site. The chain and dotted lines are the NCA curves for $\Gamma_{\mu SR}$ assuming a trigonal distortion (the B_2^0-term) of the Yb site due to the μ^+-charge, with respectively $B_2^0 = -1.57$ K and $B_2^0 = -2.35$ K.

The dynamical susceptibility for a Kondo ion with a crystal field has been computed using a perturbative approach in the self-consistent 'ladder' approximation [20] and used for comparison with inelastic neutron spectra for Ce compounds. In this section, we present the results of the calculation of $\chi''(\omega)$ using the NCA formalism in the presence of a cubic

CEF interaction, and obtain the thermal variations of $\Gamma_{\mu SR}$ and Γ_Q which we compare with the experimental data.

The NCA calculation in the presence of CEF splittings follows the same lines as in reference [3], but with three pseudo-fermion spectral densities associated with the three CEF states with their degeneracies. The input parameters for the one-impurity Anderson Hamiltonian are (in units of the bandwidth D): the position of the 4f level below the Fermi level $\epsilon_f = -0.9$, the bare hybridization width Γ_h = 0.05 and the energies of the CEF levels; the resulting 4f-shell occupation number at $T = 0$ is n_f = 0.98, i.e. the calculation is done in the scaling (or Kondo) regime. The Kondo temperature T_0 is obtained from the approximate formula

$$T_0 = D\left(\frac{\Gamma_h}{\pi|\epsilon_f|}\right)^{1/N_f} \exp\left(-\frac{\pi|\epsilon_f|}{N_f\Gamma_h}\right). \tag{11}$$

The inelastic neutron spectra were obtained using the relation for the neutron cross section $S(\omega)$:

$$S(\omega) = \frac{\hbar}{\pi}\frac{1}{(g_J\mu_B)^2}\frac{1}{1-\exp(-\hbar\omega/k_BT)}\chi''(\omega). \tag{12}$$

The quasi-elastic width and the inelastic position and width were obtained by fitting $S(\omega)$ with Lorentzian-shaped lines. The μSR dynamical width was obtained using equation (6). The calculated 4f excitation spectra at selected temperatures are presented in figure 7. The Kondo temperature was set at T_0 = 20 K. This particular value was chosen because it approximately reproduces the experimental thermal variation of the quasi-elastic width Γ_Q, as seen in figure 8 (the dashed line). The $\sqrt{T}$-like behaviour is obtained, contrary to the case of the kf exchange interaction which yields a linear Korringa-like variation (see figure 6), but the NCA calculation somewhat underestimates Γ_Q at high temperature. The NCA calculation satisfactorily reproduces the observed shift of the inelastic line towards lower energy as temperature increases [12], which represents the renormalization of the crystal-field interaction by the hybridization, but again underestimates the inelastic width at high temperature. The calculated thermal variation of $\Gamma_{\mu SR}$ obtained with $T_0 = 20$ K is shown in figure 8 as a solid line. Although it reproduces the overall experimental trend, with a $\sqrt{T}$-like saturation at high temperature, it is markedly higher than the experimental data below 150 K.

The NCA calculation of the 4f excitation spectra in the presence of CEF splittings therefore approximately accounts for the inelastic neutron spectra in $YbAuCu_4$ with a Kondo temperature $T_0 = 20$ K. The dynamical μSR linewidth, however, is not reproduced correctly at low temperature. Some reasons for this discrepancy are discussed in section 5. We shall first examine the influence of a perturbation of the crystal field acting on the Yb^{3+} ion due to the presence of the μ^+-charge (subsection 5.1). Next we will discuss other possible reasons for the observed discrepancy (subsection 5.2). Finally we will comment on the relationship between the two Kondo temperature scales (subsection 5.3).

5. Discussion of the results

5.1. The crystal-field perturbation induced by the μ^+-charge

The presence of the μ^+-charge at an interstitial site close to the rare-earth ion can create a sizeable distortion of the crystal field at the rare-earth site. The importance of this effect has been recently demonstrated, for the intermetallic compound $PrNi_5$, by μSR Knight shift measurements [21]. The crystal-field distortion can modify the wave-functions and the level

splittings of the rare-earth ion during the muon lifetime. This in turn can modify the 4f spectral function $S(\omega)$ given by equation (12) and therefore $\Gamma_{\mu SR}$ given by equation (6). In $YbAuCu_4$, we deduced that the most probable muon stopping site is the 4d site (see section 3). This means that the muon is located at a distance $a\sqrt{3}/4$ from the Yb ion along the cubic (111) direction. We thus introduced an axial distortion along the (111) direction in the CEF Hamiltonian:

$$\mathcal{H}_{CEF} = \mathcal{H}_{cub} + B_2^0[3J_z^2 - J(J+1)] \tag{13}$$

where $\mathcal{H}_{cub}$ is the standard cubic term and Oz the (111) axis. For different reasonable values of B_2^0 we computed $\Gamma_{\mu SR}(T)$ using the NCA formalism with T_0 = 20 K. We found that a positive B_2^0 has a negligible effect on the values of $\Gamma_{\mu SR}$. Selected curves with a negative B_2^0 are shown in figure 8: $B_2^0 = -1.57$ K (the chain line) and $B_2^0 = -2.35$ K (the dotted line). The agreement between the experimental $\Gamma_{\mu SR}(T)$ data and the NCA curve with the $B_2^0 = -2.35$ K distortion is better than with the NCA curve with cubic symmetry (the solid line in figure 8), especially below 150 K. Such a distortion leads to a CEF ground state close to the $|J = 7/2; J_z = \pm 7/2\rangle$ pure state, and to CEF splittings of 0 K, 69 K, 93 K and 115 K (the distortion lifts the Γ_8 fourfold degeneracy). Using a point charge model, we find that the value $B_2^0 = -2.35$ K is reproduced assuming an effective charge Z_{eff} = 0.15e for the μ^+, which seems reasonable (e is the opposite of the electron charge). The Hamiltonian (13) cannot however be considered as exact, because the presence of the μ^+-charge is expected to lead to small displacements of the neighbouring atoms and to a rearrangement of the conduction electron screening clouds. Therefore, the coefficients of the cubic term $\mathcal{H}_{cub}$ can be also modified. The NCA curve can be made to stick closer to the experimental data by somewhat increasing $|B_2^0|$ and by slightly decreasing the value of Δ_e used to derive $\Gamma_{\mu SR}$, according to equation (5). However, due to the approximation inherent to the Hamiltonian given as equation (13), we do not think such a procedure is reliable.

The present calculation must be considered as a model calculation showing the strong influence of a μ^+-induced distortion on the values of $\Gamma_{\mu SR}$. Therefore, the μ^+-induced distortion of the local crystal field appears to be an important ingredient for a quantitative understanding of the μSR data in $YbAuCu_4$. We think that it can account for the major part of the deviation between the $\Gamma_{\mu SR}$ data and the NCA calculation with a cubic Yb^{3+} site. Confirmation of the importance of this effect could be obtained by performing μSR Knight shift measurements [21] for $YbAuCu_4$. The unusual thermal variation observed for the mean nuclear dipole coupling Δ_n (see subsection 2.3) could also arise from the presence of a strong μ^+-induced electric field gradient at the sites of the quadrupolar nuclei ^{63}Cu ($I = 3/2$), ^{65}Cu ($I = 3/2$), ^{173}Yb ($I = 5/2$) and ^{197}Au ($I = 3/2$).

5.2. Other possible mechanisms for the deviation of the μSR dynamical width data from the NCA curve

The $\Gamma_{\mu SR}$ values are derived from the experimental λ_Z-values through the formula given as equation (5), which involves the 4f–muon spin coupling Δ_e. The latter was estimated to be $\simeq$208 MHz, from a calculation taking into account the dipolar coupling only. This value of Δ_e corresponds to a mean dipolar field of 245 mT. There is also a transferred hyperfine 4f–muon coupling, the value of which is unknown. The fact that the experimental data and the NCA prediction are in agreement at high temperature is an indication that the transferred hyperfine field is probably not very large. Knight shift measurements at high field could allow us to determine the hyperfine coupling constant, which is expected to be temperature

independent. In any case, the constant of proportionality between λ_Z and $\Gamma_{\mu SR}^{-1}$ is expected to be temperature independent, and taking into account a transferred hyperfine field would not explain the discrepancy between the NCA calculation and experiment.

Alternatively, one could invoke the inadequacy of the NCA for describing a Kondo ion in the presence of a crystal field, at least for the case where the Kondo temperature T_0 is of the same order of magnitude as the CEF splittings. We have seen however that the inelastic neutron scattering spectra are rather satisfactorily accounted for by the NCA calculation at low temperature, as regards the dynamical widths and the inelastic line position. Therefore, we think that the small deviations observed between the NCA calculation of the 4f excitation spectra and the experimental neutron data are not sufficient to explain the large discrepancy for the $\Gamma_{\mu SR}$ values.

We notice in figure 8 that the experimentally derived low-temperature $\Gamma_{\mu SR}$ values are of the same magnitude as the quasi-elastic neutron width Γ_Q. This is in contradiction with our calculations using either the *k*f exchange [16] or the present Anderson model, which predict that the ratio $\Gamma_{\mu SR}/\Gamma_Q$ is of the order of magnitude of 2 or 3 at low temperatures. The experimental $\Gamma_{\mu SR}$ values appear to be underestimated, which means that the λ_Z-contribution coming from the 4f fluctuations is overestimated. In figure 4 we have plotted as a dashed line the $\lambda_Z(T)$-values expected if $\Gamma_{\mu SR}(T)$ follows the theoretical NCA curve. For instance, at $T = 40$ K, the λ_Z-value that would yield the NCA $\Gamma_{\mu SR}$ value is almost four times smaller than the measured value. Consequently, there would be an extra contribution to the exponential depolarization rate, which is important at low temperature and which vanishes above ∼100 K–150 K. We discuss here two phenomena which could account for this extra component, which seemingly has no detectable effects on the neutron scattering spectra.

First, the NCA scheme neglects the magnetic correlations between Yb^{3+} ions at different sites. Short-range intersite correlations between the CEF excitations can persist far into the paramagnetic regime, as is evident for example in $ErAl_2$, where they have been detected by μSR spectroscopy at up to ∼10 times the Curie temperature [22]. In our case they would have to exist to up to ∼300 times the Néel temperature, which seems unrealistic. In the inelastic neutron scattering spectra of $YbAuCu_4$ [12], a Gaussian-shaped quasi-elastic line, indicative of magnetic correlations, is observed below 10 K, i.e. for $T < 10T_N$. Therefore the presence of short-range correlations does not seem to account for this extra component to λ_Z at high temperature.

Recently a quantum mechanical duality model for strongly correlated electronic systems has been introduced [23]. In this model the low-energy excitations contain a localized spin-fluctuation part which is coupled to the itinerant-fermionic part. Most of the spectral weight of 4f electrons is dominated by the localized component. Experimental support for this picture of two different substates has been presented from μSR and bulk measurements on uranium and cerium compounds [24, 25, 26, 27]. Because of the form factor and the small spectral weight associated with it, it is probably difficult to detect the itinerant component by neutron scattering. On the other hand the muon, being localized in an interstitial site, is an ideal microscopic tool for its investigation. We are looking for a source of depolarization with a damping rate of ∼0.12 MHz at 20 K. Although up to now the only reported high-temperature μSR signature of the itinerant component is characterized by a much smaller damping rate ($\lambda_Z \simeq 0.003$ MHz for $CeRu_2Si_2$; reference [27]), we suggest that the difference between the NCA prediction and the measured λ_Z could be accounted for by the itinerant 4f-electron component of the duality model of Kuramoto and Miyake [23]. In this interpretation the decrease of the related damping rate as temperature increases is attributed to the reduction of the amplitude of the fluctuations.

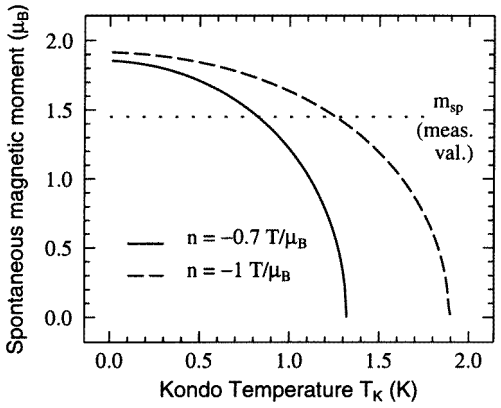

Figure 9. The dependence of the $T = 0$ K Yb^{3+} spontaneous magnetic moment m_{sp} on the 'low-temperature' Kondo scale T_K. The two curves, which are calculated using the variational solution of the Kondo problem, correspond to the lower and upper values of the molecular-field constant estimated in reference [11]. The dotted line indicates the measured value of m_{sp}. From this figure we deduce the 'low-temperature' Kondo scale for $YbAuCu_4$: $T_K = 1.0(2)$ K.

5.3. The high- and low-Kondo-temperature scales

The Kondo energy scale $k_B T_0$ appearing in the NCA calculation of section 4 relates in principle to the 'high-temperature' Kondo properties. It is renormalized by any interaction that splits the N_f degenerate ionic levels (magnetic field, crystal electric field). For describing the low-temperature properties, another energy scale $k_B T_K$ is relevant, linked to $k_B T_0$ by the following expression, obtained through the variational solution of the Kondo problem at $T = 0$ [28, 29]:

$$\prod_m (\Delta_m + k_B T_K) = (k_B T_0)^{N_f}. \tag{14}$$

For the case of $YbAuCu_4$: $\Delta_1(\Gamma_7)/k_B = 0$; $\Delta_2(\Gamma_8)/k_B = \Delta_3(\Gamma_8)/k_B = 45$ K; $\Delta_4(\Gamma_6)/k_B = 80$ K, which yields

$$T_0 = (T_K \Delta_2^2 \Delta_4 / k_B^3)^{1/4} \simeq \alpha {T_K}^{1/4} \tag{15}$$

where $\alpha = 20$ $K^{3/4}$, and where we have neglected T_K with respect to Δ_2/k_B, Δ_3/k_B and Δ_4/k_B. The Kondo scale $k_B T_K$ rules the low-temperature anomalous properties linked with the competition between the RKKY interaction and the Kondo screening of the magnetic moment [30]. It is of interest to check whether the above determination of T_0 is compatible with the T_K-value obtained from the spontaneous-moment reduction [11]. Indeed, using the variational solution of the Kondo problem, it is possible to compute the $T = 0$ spontaneous moment m_{sp} as a function of T_K, in the molecular-field approximation [29]. The $m_{sp}(T_K)$-curves, obtained for the two limiting values of the molecular-field constant n as estimated for the Yb^{3+} sublattice in $YbAuCu_4$ [11], are represented in figure 9. $m_{sp}(T_K)$ is seen to decrease as the Kondo temperature increases, i.e. as the Kondo coupling progressively overcomes the RKKY exchange interaction. We deduce that the value of T_K accounting for the observed reduced spontaneous moment is $T_K = 1.0(2)$ K [31]. The 'high-temperature' T_0-value obtained from equation (15) is then: $T_0 \sim 20$ K, in good agreement with the value determined in section 4.

6. Summary

Our μSR study of the cubic Kondo lattice $YbAuCu_4$ in the temperature range 0.1 K–280 K, in longitudinal fields of 0 and 20 mT, exhibits two temperature ranges as regards the temporal decay of the muon polarization. The spectra at low temperature, showing a complex behaviour, could not be analysed in detail. Qualitatively, the depolarization rate shows an anomaly at around 0.5 K which is associated with the onset of magnetic ordering of the Yb^{3+} sublattice. At high temperature the zero-field spectra are depolarized mainly by the quasi-static magnetic field distribution of the nuclear magnetic moments. The muon is static and seems to be localized in site 4d of the fcc structure over the whole temperature range investigated. Surprisingly we find that the width of the dipolar field at the muon site produced by the nuclear moments is temperature dependent. Above 20 K, application of a longitudinal field decouples the nuclear dipole system from the muon spins and the signal recovers an exponential form; the muon depolarization originates thus from the paramagnetic fluctuations which, in $YbAuCu_4$, are dominated by the coupling of the 4f moments with the conduction electron spins.

A first analysis of the dynamical quasi-elastic neutron and μSR linewidths, assuming that the 4f fluctuations are due to the standard kf exchange interaction, is not satisfactory. In order to take into account the Kondo coupling on the Yb^{3+} ion, we performed a calculation using the non-crossing approximation (NCA) scheme for the solution of the Anderson one-impurity Hamiltonian, in the presence of the cubic crystal-field interaction on the Yb^{3+} ion. On one hand, we find that the inelastic neutron spectra are approximately reproduced by the NCA dynamical susceptibility, with a Kondo temperature $T_0 = 20$ K, in good agreement with the 'low-temperature' Kondo scale value $T_K \simeq 1$ K, after renormalization by the crystal-field interaction. On the other hand, the observed dynamical μSR linewidth, proportional to $\chi''(\omega)/\omega$ for $\omega \to 0$, can only be accounted for by the NCA calculation at high temperature, assuming a cubic site for the Yb^{3+} ion. A model NCA calculation including a μ^+-induced axial distortion of the Yb site improves the agreement between the experimental $\Gamma_{\mu SR}$ data and the theoretical curve, suggesting that the distortion of the Yb cubic site by the μ^+-charge plays an important role. We have discussed other possible reasons for the discrepancy between the NCA prediction and the μSR results. A possible method that could help to select between these reasons is that of comparing μSR Knight shift data with macroscopic magnetic susceptibility. If the relationship between the results of these techniques was found to be temperature independent, then one could safely conclude that the effect of the muon charge on the CEF levels is negligible. In addition, the μSR Knight shift would allow one to determine the hyperfine coupling constant.

Acknowledgments

We thank the ISIS facility crew for the excellent working conditions, S R Brown for his help during the data collection and A P Murani for providing the $YbAuCu_4$ sample. The researchers from the Netherlands acknowledge support from the Dutch Scientific Organization (NWO). The μSR measurements were partly supported by the Commission of the European Community through the Large Installations Plan.

We also thank M J Besnus, from Strasbourg University (France), for providing us with her unpublished low-temperature specific heat data for $YbAuCu_4$.

References

[1] Karlsson E B 1995 *Solid State Phenomena as Seen by Muons, Protons and Excited Nuclei* (Oxford: Clarendon) Schenck A and Gygax F N 1995 *Handbook of Magnetic Materials* vol 9, ed K H J Buschow (Amsterdam: Elsevier Science)

[2] Brandt N B and Moshchal'kov V V 1984 *Adv. Phys.* **33** 373

[3] Cox D L, Bickers N E and Wilkins J W 1985 *J. Appl. Phys.* **57** 3166

[4] Murani A P, Knorr K, Buschow K H J, Benoit A and Flouquet J 1980 *Solid State Commun.* **36** 523

[5] Loidl A, Knopp G, Spille H, Steglich F and Murani A P 1989 *Physica* B **156+157** 794

[6] Benakki M, Kappler J P and Panissod P 1987 *J. Phys. Soc. Japan* **56** 3309

[7] Qachaou A, Beaurepaire E, Benakki M, Lemius B, Kappler J P, Meyer A J P and Panissod P 1987 *J. Magn. Magn. Mater.* **63+64** 635 and references therein

[8] Barth S, Ott H R, Gygax F N, Hitti B, Lippelt E, Schenk A, Baines C, B. van den Brandt, Konter T and Mango S 1987 *Phys. Rev. Lett.* **59** 2991

[9] Amato A 1994 *Physica* B **199+200** 91

[10] Rossel C, Yang K N, Maple M B, Fisk Z, Zirngiebel E and Thompson J D 1987 *Phys. Rev.* B **35** 1914

[11] Bonville P, Canaud B, Hammann J, Hodges J A, Imbert P, Jéhanno G, Severing A and Fisk Z 1992 *J. Physique* I **2** 459

[12] Severing A, Murani A P, Thompson J D, Fisk Z and Loong C K 1990 *Phys. Rev.* B **41** 1739

[13] Eaton G H, Scott C A and Williams W G 1994 *Hyperfine Interact.* **87** 1099

[14] Noakes D R, Ismail A, Ansaldo E J, Brewer J H, Luke G M, Mendels P and Poon S J 1995 *Phys. Lett.* **199A** 107

[15] Hartmann O 1977 *Phys. Rev. Lett.* **39** 832

[16] Dalmas de Réotier P, Yaouanc A and Bonville P 1996 *J. Phys.: Condens. Matter* **8** 5113

[17] Kasuya T 1956 *Prog. Theor. Phys.* **16** 45

[18] Slichter C P 1965 *Principles of Magnetic Resonance* (New York: Harper and Row)

[19] Besnus M J, Braghta A, Hamdaoui N and Meyer A 1992 *J. Magn. Magn. Mater.* **104–107** 1385

[20] Maekawa S, Takahashi S, Kashiba S and Tachki M 1985 *J. Phys. Soc. Japan* **54** 1955

[21] Feyerherm R, Amato A, Grayevsky A, Gygax F N, Kaplan N and Schenk A 1995 *Z. Phys.* B **99** 3

[22] Hartmann O, Kalsson E, Wäppling R, Chappert J, Yaouanc A, Asch L and Kalvius G M 1986 *J. Phys. F: Met. Phys.* **16** 1593

[23] Kuramoto Y and Miyake K 1990 *J. Phys. Soc. Japan* **59** 2831

[24] Schenck A, Birrer P, Gygax F N, Hitti B, Lippelt E, Weber M, Böni P, Ficher P, Ott H R and Fisk Z 1990 *Phys. Rev. Lett.* **65** 2454

[25] Caspary R, Hellmann P, Keller M, Sparn G, Wassilew C, Köhler R, Geibel C, Schank C, Steglich F and Phillips N E 1993 *Phys. Rev. Lett.* **71** 2146

[26] Feyerherm R, Amato A, Gygax F N, Schenck A, Geibel C, Steglich F, Sato N and Komatsubara T 1994 *Phys. Rev. Lett.* **73** 1849

[27] Amato A, Feyerherm R, Gygax F N, Schenck A, Flouquet J and Lejay P 1994 *Phys. Rev.* B **50** 619

[28] Gunnarsson O and Schönhammer K 1983 *Phys. Rev.* B **28** 4315

[29] LeBras G 1994 *Thesis* Orsay–Paris XI University

[30] Doniach S 1977 *Physica* B **91** 231

[31] The T_K-value derived previously [11] (0.3 K) is underestimated due to an erroneous account of the renormalization of the Kondo temperature with respect to the exchange field.